THE ASTROPHYSICAL JOURNAL, 452:164–176, 1995 October 10

PROBLEMS WITH COLD CLOUDS IN COOLING FLOWS

G. MARK VOIT[1]
Department of Physics and Astronomy, The Johns Hopkins University, Baltimore, MD 21218
AND
MEGAN DONAHUE
Space Telescope Science Institute, 3700 San Martin Drive, Baltimore, MD 21218
Received 1994 November 28; accepted 1995 April 20

ABSTRACT

Some X-ray observations of cooling-flow clusters show soft X-ray absorption exceeding that expected along the line of sight through our own Galaxy. This absorption appears at the position of the cooling flow and covers a similar solid angle at the center of the cluster. The inferred absorbing column densities correspond to a hydrogen mass exceeding $10^{11}\ M_\odot$, prompting suggestions that the absorbing material is condensed gas accumulated from the cooling flow. We explore the characteristics of cold atomic clouds embedded in an X-ray–emitting cooling flow and find that, if they cover the central 100 kpc of the cluster, they should already have been detected in H I 21 cm emission. Dust in cooling-flow clouds can catalyze molecule formation, making them unobservable at 21 cm, but dusty molecular clouds should radiate detectable, optically thick CO rotational lines, which likewise have not been seen. X-ray transient heating of grains prohibits most of the CO from condensing onto grain surfaces and thus ensures that the CO lines are optically thick. Ionized X-ray–absorbing gas would radiate profusely in optical, UV, or X-ray emission lines. We report limits on Hα and [Fe X] 6374 Å surface brightnesses from deep long-slit spectroscopy that rule out ionized columns thicker than 10^{21} cm^{-2} and cooler than 1.5×10^6 K. Limits on O VIII Lyα do not allow the X-ray–absorbing gas to be at higher temperatures.

One remaining possibility is that dust in the hot intracluster medium absorbs the soft X-rays. The soft X-ray opacity of dust is similar to its optical opacity. Optical extinctions inferred from the deficits of background galaxies and quasars counted behind clusters might be consistent with the dust column densities inferred from soft X-ray absorption. If dust is the culprit, limits on the 100 μm luminosities of clusters imply that the dust-to-gas ratio must be higher at ~1 Mpc, at which large grains can survive for longer than 10^9 yr, than in the cores of clusters, where sputtering destroys grains on a much shorter timescale. However, dust at ~1 Mpc in quantities sufficient to produce significant soft X-ray absorption represents a large fraction of the total metal content of a cluster. Submillimeter continuum observations should eventually determine whether dust is widespread in the intracluster media of clusters of galaxies.

Subject headings: cooling flows — dust, extinction — galaxies: clusters: general — intergalactic medium — X-rays: galaxies

1. INTRODUCTION

The X-ray–emitting gas at the centers of many clusters of galaxies can cool in less than a Hubble time. When this fact was first noticed, it seemed natural that the intracluster medium (ICM) in such clusters should flow gradually toward the cluster center as its inner regions cooled and condensed in a "cooling flow" (Fabian & Nulsen 1977; Cowie & Binney 1977; see Fabian 1994 for a review). In the intervening years, many investigators have tried, and failed, to identify the cooled gas once it has dropped below the threshold of X-ray observability. A cooling flow of $\sim 10^2\ M_\odot$ yr^{-1} deposits $10^{12}\ M_\odot$ within the central 100 kpc of a cluster over a Hubble time. Normal star formation appears to occur at no more than 10% of this rate (Fabian 1994). Recombination line luminosities limit the total mass of 10^4 K ionized hydrogen to less than $10^8\ M_\odot$ (Heckman et al. 1989). Atomic 21 cm observations limit the total mass of optically thin H I to less than 10^{10}–$10^{11}\ M_\odot$ (McNamara, Bregman, & O'Connell 1990; hereafter MBO), and carbon monoxide observations limit the mass in clouds similar to Galactic molecular clouds to less than 10^9–$10^{10}\ M_\odot$ (O'Dea et al. 1994; hereafter OBMTS). If cooling flows exist, the ultimate mass sink is virtually undetectable.

Soft X-ray spectroscopy of clusters has suggested a possible solution to this "mass sink problem." The X-ray–absorbing columns toward many clusters of galaxies exceed those expected from Galactic absorption alone. The amounts of excess absorption measured by White et al. (1991) with the *Einstein* Solid State Spectrometer indicate cool hydrogen columns of 10^{20}–10^{21} cm^{-2} that appear to correlate with the magnitudes of the cooling flows in these clusters. Since these two parameters can amplify one another in simultaneous fits, this apparent correlation should be interpreted cautiously. Allen et al. (1993), using the *ROSAT* Position Sensitive Proportional Counter (PSPC), have thoroughly studied the cluster Abell 478, the most heavily self-absorbed in the White et al. (1991) sample. The cool temperature and high brightness of the X-ray gas at the center of Abell 478 indicate that this cluster harbors a large cooling flow, the spectrum of which complicates the analysis of soft X-ray absorption. Allen et al. find that excess absorption equivalent to a hydrogen column density $\gtrsim 10^{21}$ cm^{-2} covers the central 200 kpc of the cluster. Since the absorption appears to be centered on the cluster, its origin is unlikely to be Galactic. The total amount of cool absorbing

[1] Hubble Fellow.

mass implied exceeds $10^{12}\ M_\odot$. Cooling-flow proponents have argued that this X-ray–absorbing material, in some very cold and difficult to detect gaseous form, is the long-sought mass sink for cooling flows (White et al. 1991; Daines, Fabian, & Thomas 1994; Ferland, Fabian, & Johnstone 1994, hereafter FFJ).

Cool clouds with the column density and covering factor required to produce the X-ray self-absorption have still not been detected in any other band (Jaffe 1992; OBMTS; Antonucci & Barvainis 1994; McNamara & Jaffe 1994; Braine et al. 1995). Intracluster clouds are least detectable when they are cold and molecular, but the absorbed X-ray power, which can reach several times 10^{43} ergs s^{-1}, must reemerge somewhere in the electromagnetic spectrum. Two recent calculations evaluating the temperatures and emission-line fluxes expected from X-ray–irradiated molecular gas (OBMTS; FFJ) have arrived at conflicting conclusions about the detectability of cold, X-ray–absorbing clouds in cooling flows. The cloud temperatures predicted by OBMTS imply that the covering factor of cold clouds must be $\ll 1$. The models of FFJ predict much colder clouds that can potentially evade detection even if they completely cover the cluster core.

This paper investigates whether cold, X-ray–irradiated clouds covering the inner 100–200 kpc of cooling-flow clusters can indeed escape current infrared, submillimeter, and radio limits. Section 2 outlines the thermal and chemical structure of such clouds, which can be either atomic or molecular, depending on the amount of dust they contain. The current H I 21 cm limits, discussed in § 3, imply that if cold, absorbing clouds cover the cooling-flow region, they must be mostly molecular and therefore dusty. Section 4 demonstrates that CO emission from molecular intracluster clouds should already have been detected if the clouds have a high enough covering factor to produce the X-ray absorption. Section 5 discusses whether X-ray absorption can arise in the hot ICM and evaluates one remaining possible source of X-ray opacity, dust grains in the outer parts of the cluster.

2. COLD CLOUDS IN THE ICM

Whatever blocks the soft X-rays in cooling-flow clusters absorbs a dilute but hard X-ray spectrum. In a steady state, the obscuring objects must reradiate a flux identical to the one absorbed. Cool clouds in pressure equilibrium with the hot gas at a radius of 100 kpc in a 100 $M_\odot$ yr^{-1} cooling flow intercept X-ray radiation so dilute that the clouds remain mostly neutral. Within the cloud, as the ionizing radiation attenuates, deeper layers are progressively cooler, and the collisionally excited emission lines that reemit the absorbed X-ray energy belong to the far-infrared, submillimeter, and radio bands. This section examines the physical processes that govern the behavior of cold, X-ray–irradiated gas, in order to determine the emission-line fluxes from the surfaces of cooling-flow clouds. We first explore X-ray energy deposition into neutral gas and identify the relevant cooling mechanisms. Then we sketch the thermal structure of cooling-flow clouds, assess their line-emitting properties, and explain why the calculations of FFJ and OBMTS disagree.

2.1. *X-Ray Energy Deposition*

Following FFJ, we construct an incident spectrum assuming $(100\ M_\odot\ \mathrm{yr}^{-1})\dot{M}_{100}$ cools from $10^{7.8}$ K to low temperatures within a cooling radius of $(100\ \mathrm{kpc})r_{100}$. The X-ray flux at this radius is $(1.0 \times 10^{-4}\ \mathrm{ergs\ cm^{-2}\ s^{-1}})\dot{M}_{100} r_{100}^{-2}$, with roughly equal power per logarithmic frequency interval from 100 eV to 10 keV (FFJ).[2] The spectral energy flux thus follows the approximate form $F_E \sim (2.2 \times 10^{-5}\ \mathrm{ergs\ cm^{-2}\ s^{-1}})E^{-1}$, where E is the photon energy. The requirement that the cooling time be of order one Hubble time at the cooling radius implies an ambient hydrogen density $\sim 2 \times 10^{-3}$ cm^{-3}. Clouds at 10^4 K in pressure equilibrium with the cooling flow at r_{100} then have ionization parameters $U \sim 10^{-6.5}$–$10^{-7.5}$, where U is the ionizing photon density divided by the total hydrogen density ($n_{\rm H}$) at the cloud's surface.[3] These clouds will therefore be mostly neutral, with fractional ionization dropping into the cloud as the X-rays abate.

Most of the absorbed X-rays photoionize the inner shells of metals, so X-ray energy deposition into cooling-flow clouds varies linearly with the total metallicity. Cold clouds of solar abundances and total hydrogen column density $N_{\rm H}$ have keV optical depths $\sim (N_{\rm H}/4 \times 10^{21}\ \mathrm{cm^{-2}})(E/1\ \mathrm{keV})^{-2.5}$. Since intracluster media appear to have metallicities ~ 0.3 solar, FFJ assumed metal abundances in cooling-flow clouds were similar. At these lower metallicities, even higher $N_{\rm H}$ is needed to produce the observed absorption.

Combining the two approximations for spectral energy flux and X-ray optical depth yields a useful expression for the local energy deposition rate per hydrogen nucleus at a column depth $N_{\rm H}$ inside a cooling-flow cloud,

$$H_{\rm dep}(N_{\rm H}) \sim (8.8 \times 10^{-27}\ \mathrm{ergs\ s^{-1}})\left(\frac{N_{\rm H}}{10^{21}\ \mathrm{cm^{-2}}}\right)^{-1} \dot{M}_{100} r_{100}^{-2}\ . \quad (1)$$

Since $F_E \propto E^{-1}$, changes in metallicity do not strongly affect $H_{\rm dep}$, which depends primarily on the power-law index of the absorption cross section per H atom and only weakly on its normalization. This formula reproduces the X-ray energy deposition rates calculated by a CLOUDY photoionization model (Ferland 1993) with FFJ parameters to within a factor of 2 from $N_{\rm H} = 10^{19}$ to $10^{21.5}$ cm^{-2}. Not all of this energy goes into heating the gas. Most of the X-ray photoelectrons created within grains fail to escape, heating the grains instead. For Galactic depletions and grain sizes, a fraction $f_g \sim \frac{1}{2}$ of the energy absorbed from ~ 1 keV X-rays goes into grain heating (Voit 1991b).

X-ray photoelectrons ejected from gas-phase atoms and those that escape grains heat neutral gas inefficiently. These fast electrons transfer their energy mostly by ionizing and exciting H, He, and H_2 through a cascade of secondary ionization electrons. In atomic gas of low ionization ($X_e \equiv n_e/n_{\rm H} < 10^{-3}$), X-ray photoelectrons deposit 10%–15% of their energy as heat (e.g., Xu & McCray 1991). The remainder converts into H and He line emission. The heating rate per H nucleus in atomic cooling-flow clouds is then

$$H_{\rm heat,H^0}(N_{\rm H}) \sim (1.1 \times 10^{-27}\ \mathrm{ergs\ s^{-1}})\left(\frac{N_{\rm H}}{10^{21}\ \mathrm{cm^{-2}}}\right)^{-1} \times (1 - f_g)\dot{M}_{100} r_{100}^{-2}\ . \quad (2)$$

X-ray heating in molecular clouds is more efficient. About 40% of the X-ray photoelectric energy ionizes H_2 (Cravens, Victor,

[2] Even if the ICM is not actually cooling and flowing, this expression still adequately describes the flux at 100 kpc in a "cooling-flow" cluster.

[3] Ionization parameters of cooling-flow clouds within 10 kpc of the cluster center can potentially be much higher (Donahue & Voit 1991; Voit, Donahue, & Slavin 1994).

& Dalgarno 1975; Voit 1991a), which recombines through the reactions

$$H_2^+ + H_2 \rightarrow H_3^+ + H ,$$
$$H_3^+ + e^- \rightarrow H_2 + H ,$$
$$\rightarrow 3H ,$$

(Henry & Lane 1969). The 11 eV of recombination energy left over after dissociation passes mostly into heat, but some is radiated away in H_3^+ vibrational lines (Glassgold & Langer 1973). Here we follow Glassgold & Langer (1973) and assume an overall X-ray heating efficiency of $\frac{1}{3}$ in molecular gas, so

$$H_{\rm heat,H_2}(N_{\rm H}) \sim (2.9 \times 10^{-27} \text{ ergs s}^{-1})\left(\frac{N_{\rm H}}{10^{21} \text{ cm}^{-2}}\right)^{-1} (1-f_g)\dot{M}_{100} r_{100}^{-2} . \quad (3)$$

Note that the heating rate per H_2 molecule is $2H_{\rm heat,H_2}$.

2.2. *Chemical Structure*

X-rays that penetrate deeply into a cold cloud produce multiple ionization and dissociation events per photon. Dust in the cloud catalyzes molecule formation, helps block dissociating UV radiation, and accretes metals from the gas phase. Together X-rays and dust determine the chemical structure of cooling-flow clouds. The following paragraphs outline ionization balance, molecular balance, and dust formation processes in these clouds.

2.2.1. *Ionization Balance*

In both atomic and neutral gas for which $X_e < 10^{-2}$, $\sim$40% of the X-ray photoelectric energy deposited into the gas phase goes into ionization of H or H_2 (Xu & McCray 1991; Voit 1991a). The ionization rate per hydrogen atom in neutral gas is $\sim 0.4 H_{\rm dep}/(13.6 \text{ eV})$, and the ionization rate per molecule in molecular gas is $\sim 0.8 H_{\rm dep}/(15.4 \text{ eV})$. At low cloud temperatures ($T_{\rm cl} \lesssim 100$ K), ionized hydrogen recombines at the rate $(3.0 \times 10^{-11} \text{ cm}^3 \text{ s}^{-1}) n_e T_{c10}^{-0.6}$, where T_{c10} is the cloud temperature in units of 10 K (Ferland 1993). Near a column depth $N_{\rm H} \sim 10^{19}$ cm^{-2} in an atomic cloud, the fractional ionization is thus

$$X_e \sim 10^{-4}\left(\frac{N_{\rm H}}{10^{19} \text{ cm}^{-2}}\right)^{-1/2} T_{c10}^{0.8} \dot{M}_{100}^{1/2} r_{100}^{-1} , \quad (4)$$

so nonthermal electron cascade dominates X-ray energy deposition. In deeper layers, photoionization of C and Si dominates the supply of free electrons (FFJ).

2.2.2. *Molecular Balance*

Hydrogen molecules form on cold dust grains at the rate $(1 \times 10^{-17} \text{ cm}^3 \text{ s}^{-1}) n_{\rm H^0} T_{c10}^{1/2} \chi_d$, where χ_d is the dust-to-gas ratio in Galactic units (Hollenbach & McKee 1979). In a dust-free medium, H_2 forms primarily through the reactions (Shull & Beckwith 1982):

$$H^0 + e^- \rightarrow H^- + h\nu ,$$
$$H^- + H^0 \rightarrow H_2 + e^- .$$

FFJ include these reactions in their models of dust-free cooling-flow clouds and find that the majority of the hydrogen remains atomic to a column $N_{\rm H} = 4 \times 10^{21}$ cm^{-2}. At this depth, $\sim$30% of the H is in H_2, and $\sim$3% of the C is in CO. To become fully molecular at these column densities, cooling-flow clouds must be dusty.

X-ray dissociation of H_2 scales with the energy deposition rate. In a neutral molecular gas, aside from the 26.1 ionizations per keV of X-ray energy absorbed, there are 8.8 triplet excitations and 2.4 dissociative excitations (Voit 1991a). These events all dissociate H_2. In addition, about 10% of the 22.2 singlet excitations per keV lead to dissociation, giving a total of 39.5 dissociations per keV and an X-ray dissociation rate of

$$R_{\rm diss,H_2}(N_{\rm H}) \sim (2.2 \times 10^{-14} \text{ s}^{-1})\left(\frac{N_{\rm H}}{10^{19} \text{ cm}^{-2}}\right)^{-1} \times (1-f_g)\dot{M}_{100} r_{100}^{-2} . \quad (5)$$

Balance with H_2 formation on dust grains implies

$$\frac{n_{\rm H^0}}{2n_{\rm H_2}} \sim 0.04\left(\frac{N_{\rm H}}{10^{19} \text{ cm}^{-2}}\right)^{-1} (1-f_g)^{-1} T_{c10}^{1/2} \chi_d^{-1} \dot{M}_{100} r_{100}^{-2} . \quad (6)$$

Thus, dusty cooling-flow clouds can be highly molecular at modest column depths.

Nonionizing ultraviolet radiation from the central galaxy of the cooling flow cluster can also dissociate H_2 by exciting Lyman-Werner band (singlet) transitions; however, this radiation does not penetrate deeply enough to affect the dissociation rate in the X-ray–absorbing layers. *International Ultraviolet Explorer* observations have shown that the central galaxies in large cooling flows have 1000–2000 Å luminosities of $\sim 10^{43}$ ergs s^{-1} (Crawford & Fabian 1993), giving UV fluxes of $\sim 10^{-5}$ ergs cm^{-2} s^{-1} at the cooling radius, about 10 times the UV flux produced by the cooling ICM (FFJ) and 100 times less than the standard Habing (1968) interstellar UV field. Adopting the photodissociation coefficient for unshielded H_2 from Tielens & Hollenbach (1985) gives a UV photodissociation rate of $\sim 3 \times 10^{-13}$ s^{-1}. Although this is higher than the X-ray dissociation rate at $N_{\rm H} \sim 10^{19}$ cm^{-2}, H_2 self-shielding quickly reduces this rate to negligible levels. Since $n_{\rm H^0}/2n_{\rm H_2} \sim \chi_d^{-1}$ when UV dissociation balances H_2 formation in cooling-flow clouds at 10 K, a column $N_{\rm H} < (10^{15} \text{ cm}^{-2})\chi_d^{-1}$ suffices to drive the UV dissociation rate well below the X-ray rate (Shull 1978).

2.2.3. *Dust Formation*

Molecules form much more quickly in dusty clouds than in dust-free clouds. Since the cooling time in the hot ICM exceeds the sputtering time for submicron-sized grains by over an order of magnitude, clouds that condensed out of the hot ICM should be virtually dust free. Nevertheless, some of the gas within the central galaxies of many cooling-flow clusters appears to be dusty. Dust lanes (Sparks, Macchetto, & Golombek 1989; McNamara & O'Connell 1992) and reddening (Hu 1992) are common, and emission-line ratios indicate significant depletions of calcium (Donahue & Voit 1993). Most authors have assumed that the dusty gas came originally from a gas-rich spiral galaxy stripped of its ISM as it passed through the cluster core, perhaps merging with the central galaxy (e.g., Sparks, Macchetto, & Golombek 1989). Recently Daines et al. (1994) and Fabian et al. (1994) have suggested instead that dust might form in gas-phase reactions deep inside intracluster clouds.

The gas that red giant winds and supernovae introduce into the Galactic ISM initially contains dust. Inside cold molecular clouds, conditions are ripe for further accretion of gas-phase metals onto the original grains. Periodically, though, super-

novae drive shocks through the ISM that destroy the dust grains in a given parcel of interstellar material (e.g., Tielens et al. 1994; Jones et al. 1994). The ubiquity and regularity of ISM dust in the face of continual buffeting by shocks have led to the speculation that gas-phase processes somehow reconstruct dust in the ISM (Jura 1987; Seab 1987; Draine 1994; Jones et al. 1994).

Gas-phase processes that would create dust in cooling-flow clouds must first create the complex molecules from which dust forms. FFJ have shown that penetrating X-rays inhibit molecule formation in dust-free cooling-flow clouds. Even at depths of $N_{\rm H} \sim 4 \times 10^{21}$ cm^{-2}, only a few percent of the carbon and oxygen is in molecular form. In these models, dissociation processes operate more rapidly than molecule formation processes. Although we do not understand the gas-phase reactions that might form dust in our own interstellar medium, it appears that, in the intracluster environment, at least some dust is needed to promote the kind of rapid molecule formation that potentially produces additional dust.

Once a cooling-flow cloud has been seeded with dust grains, the amount of dust in the cloud can increase either through accretion onto existing grains or through gas-phase dust formation. If metal atoms incident on dust grains always stick, the time required to achieve $\chi_d \sim 1$ is $\sim(10^5 \text{ yr}) T_{c10}^{1/2} \chi_d^{-1}$. Hydrogen molecule formation happens only slightly faster, so this timescale can be considered the limiting one for dust formation. Matter that condenses out of the hot ICM can generate Galactic dust-to-gas ratios in $< 10^9$ yr if $\chi_d > 10^{-4}$ initially or if mixing with dust-bearing material follows condensation.

2.3. *Cooling Mechanisms*

X-ray energy deposited deep within cooling-flow clouds reemerges in a variety of channels determined by the chemical structure of the cloud. In highly neutral atomic clouds, more than 80% of the X-ray energy ionizes and excites atomic hydrogen and helium. Recombination and de-excitation reradiate this energy through the usual hydrogen recombination lines. The remaining energy, deposited directly as heat, collisionally excites the fine-structure transitions of O I, Si II, and C I, which cool the gas. In highly neutral molecular clouds, $\sim$33% of the absorbed X-ray energy passes into heat through H_2 ionization/dissociation, and $\sim$60% of the X-ray energy directly excites electronic, vibrational, and rotational transitions of H_2 and He. Thermal energy exits molecular clouds primarily in the rotational lines of CO. Far-infrared continuum emission from collisionally heated dust grains can assist in cooling both atomic and molecular gas. The next few paragraphs describe how these coolants operate in the deeper layers of cooling-flow clouds.

2.3.1. *Fine-Structure Lines*

The [O I] 63 μm, [Si II] 35 μm, and [C I] 610 μm and 370 μm lines provide most of the cooling in neutral cooling-flow clouds colder than 100 K; carbon is too neutral for [C II] 158 μm to be important (FFJ). Since the ionization level is low, collisions with H I dominate the collisional excitation rates. Figure 1 shows the optically thin cooling per H atom from these lines for FFJ abundances of O, C, and Si and collisional excitation rates from Tielens & Hollenbach (1985). The cooling per H converges at low temperatures when $n_{\rm H} \gtrsim 10^3$ cm^{-3} because the critical densities for H I collisional de-excitation of the upper levels of C I are 470 cm^{-3} and 2800 cm^{-3} (Tielens & Hollenbach 1985).

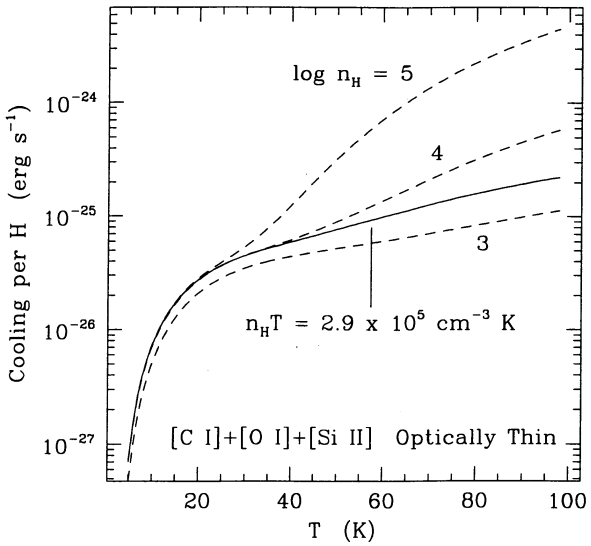

FIG. 1.—Optically thin line cooling per H atom. Cooling per H atom from the fine-structure lines of C I, O I, and Si II in an atomic gas of pressure $n_{\rm H} T = 2.9 \times 10^5$ cm^{-3} K is given. Cooling curves for gas at constant densities of 10^3, 10^4, and 10^5 cm^{-3} are also shown. These curves converge at low T when the gas density is higher than the critical densities of the C I transitions ($\sim 10^3$ cm^{-3}). As the local heating rate drops below 10^{-25} ergs s^{-1} per H atom, at $N_{\rm H} \sim 10^{19}$ cm^{-2} in atomic cooling-flow clouds, the gas temperature rapidly drops to 20 K. Optically thin cooling applies as long as the cooling lines are not thermalized.

When the C I lines become optically thick, cooling decreases. Assuming $T_{c10} \sim 1$, FFJ abundances, and thermal line widths, the optical depth of the C I 610 μm line is $\tau_{610} \sim (1.2 \times 10^{-20}$ cm$^2) T_{c10}^{1/2} N_{\rm H}$. Neutral carbon line cooling in clouds much thicker than 10^{20} cm^{-2} cannot exceed the blackbody flux in the optically thick portions of the C I lines. As the internal radiation field in the line approaches the blackbody field at the gas temperature, thermal coupling to the radiation field keeps the cloud temperature nearly constant throughout the optically thick region. Although [O I] 63 μm becomes optically thick if $\tau_{63} \sim (6.9 \times 10^{-21}$ cm$^2) N_{\rm H} > 1$, its higher critical density (4.7×10^5 cm^{-3}; Tielens & Hollenbach 1985) keeps [O I] photons from coupling strongly to the gas temperature unless $N_{\rm H} \gg 10^{21}$ cm^{-2}.

2.3.2. *Molecular Lines*

The primary coolants in molecular clouds are the CO rotational lines. Their critical densities depend on the rotational quantum number J, according to the relation $n_{\rm cr}(J) \sim (3 \times 10^3$ cm$^{-3}) T_{c10}^{-1/2} J^3$ (Hollenbach & McKee 1979), so we expect the rotational levels through $J = 2$ in molecular cooling-flow clouds to be thermally populated. Higher J levels can also be thermalized if the levels leading up to them are effectively thick (i.e., $\tau > n_{\rm cr}/n_{\rm H_2}$). If the FFJ carbon abundance is all in CO with a thermal velocity dispersion, the optical depth of the $J \rightarrow J+1$ transition is $\tau_J \sim (5 \times 10^{-19}$ cm$^{-2}) T_{c10}^{-1/2} N_{\rm H} f_J$, where f_J is the fraction of CO in level J.

Since the temperatures that determine CO level populations depend on radiative cooling, this thermal balance problem is usually solved self-consistently using escape probability methods under the assumption that temperatures throughout the cloud are uniform (Goldreich & Kwan 1974; Scoville & Solomon 1974). OBMTS modeled cooling-flow clouds using cooling functions computed by Goldsmith & Langer (1978). In deriving these cooling functions, which include secondary cool-

ants such as C I and H_2O, Goldsmith & Langer (1978) employ escape probability methods, assuming that velocity gradients within the emitting cloud are linear. Optical depths in clouds with smooth velocity gradients are proportional to the quotient of the thermal width and the velocity gradient and do not depend on position within the cloud. Thermal broadening in a static cooling-flow cloud with $N_H \sim 4 \times 10^{21}$ cm^{-2} and $n_{H_2} T_{cl} \sim 3 \times 10^5$ K creates an effective velocity gradient in CO lines of $2n_{H_2}(2\pi kT_{cl}/28m_H)^{1/2}/N_H \approx (6 \text{ km s}^{-1} \text{ pc}^{-1})T_{c10}^{-1/2}$. When $n_{CO}/n_H \approx (2.4 \times 10^{-4})T_{c10}^{-1/2}$, this velocity gradient parameter corresponds to the one used by Goldsmith & Langer (1978). Interpolating between the Goldsmith & Langer cooling functions for 10^5 cm^{-3} gas at 3 K and 10^4 cm^{-3} gas at 30 K gives a cooling rate of $(2.2 \times 10^{-28}$ ergs s$^{-1})T_{c10}^{3.2}$ per H nucleus and a corresponding molecular line flux of $(8.8 \times 10^{-7}$ ergs cm^{-2} s$^{-1})T_{c10}^{3.2}$, illustrated in Figure 2.

The models of FFJ invoke molecular line cooling functions derived by Hollenbach & McKee (1979), who also rely upon escape probability methods. Since the source function is presumed constant throughout the line-forming region, the assumption of constant temperature is implicit in these cooling functions. For a cooling-flow cloud of $N_H = 4 \times 10^{21}$ cm^{-2}, thermal line widths, and $n_{CO}/n_H = 2.4 \times 10^{-4}$, the Hollenbach & McKee (1979) CO cooling function gives $(2.4 \times 10^{-28}$ ergs s$^{-1})T_{c10}^{3.5}$ per H nucleus, corresponding to a flux of $(9.6 \times 10^{-7}$ ergs cm^{-2} s$^{-1})T_{c10}^{3.5}$. Although Hollenbach & McKee (1979) approximate various molecular parameters assuming gas temperatures exceed 100 K, their cooling rate, shown as a flux in Figure 2, does not differ much from our interpolation of the Goldsmith & Langer (1978) cooling rates.

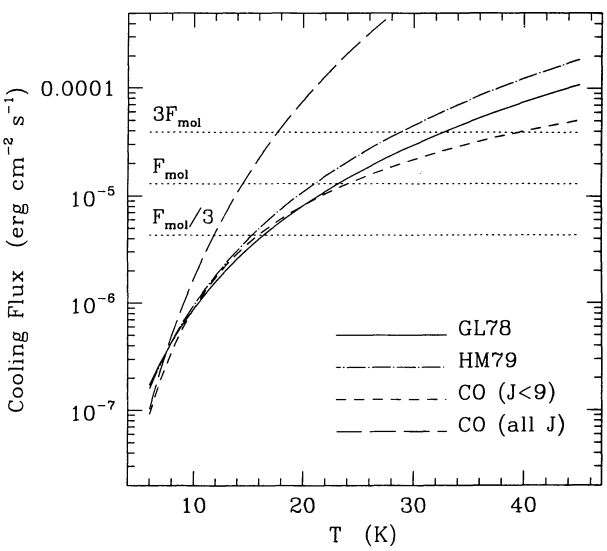

FIG. 2.—Optically thick molecular line cooling. Molecular line cooling fluxes from a 4×10^{21} cm^{-2} cloud with $n_{CO}/n_H = 2.4 \times 10^{-4}$ and thermal line widths are shown. The curve GL78 illustrates the cooling fluxes derived from Goldsmith & Langer (1978), and the curve HM79 illustrates the cooling fluxes derived from Hollenbach & McKee (1979). Also shown are total fluxes from optically thick ^{12}CO lines, summed up to $J = 8$–7 and summed over all J, with widths $\Delta v_{FWHM} = 2.355(kT_{cl}/28m_H)^{1/2}$. When the major cooling lines are optically thick, the total cooling flux depends only weakly on N_H. Dotted lines show the expected range of X-ray heating fluxes in molecular cooling-flow clouds. Equilibrium cloud temperatures when CO is optically thick range from 15 to 30 K. Even in the extreme limit in which all the ^{12}CO rotational lines are optically thick, the gas temperature still does not drop below 10 K. When supersonic turbulence broadens the CO lines, more flux can emerge in lower lying rotational transitions, reducing the equilibrium temperature but increasing the detectability of cooling-flow clouds in the CO 1–0 and 2–1 lines.

More crudely, we can estimate CO line cooling of a cooling-flow cloud by assuming all the CO lines up to a certain J are emitting at the blackbody limit. For thermal line widths, the flux in the $J \rightarrow J-1$ transition when $\tau_{J-1} \gg 1$ is

$$F_J \approx \frac{2\pi h\nu_J^4}{c^3} \frac{(\ln \tau_{J-1})^{1/2}}{e^{h\nu_J/kT_{cl}} - 1} \Delta v_{FWHM}$$

$$\approx (3.6 \times 10^{-9} \text{ ergs cm}^{-2} \text{ s}^{-1}) J^4 \frac{(\ln \tau_{J-1})}{e^{0.55J/T_{c10}} - 1} T_{c10}^{1/2} , \quad (7)$$

where $\Delta v_{FWHM} = 2.355(kT_{cl}/28m_H)^{1/2}$. Figure 2 shows total CO line cooling fluxes assuming (1) all CO rotational lines are thermalized (an extreme limit) and (2) only CO lines up to $J = 8$–7 ($n_{cr} \sim 10^6$ cm^{-3}) are thermalized (more appropriate for cooling-flow clouds). The curve-of-growth factor $(\ln \tau_{J-1})^{1/2}$ is taken to be unity in both cases. The proximity of the second curve to the more sophisticated cooling functions demonstrates that molecular cooling-flow clouds cool mainly through optically thick CO lines with $J < 9$. Because the primary cooling lines are optically thick, the total cooling flux increases slowly as N_H rises. Supersonic turbulence that broadens the lines to Δv_5 km s^{-1} increases the optically thick cooling flux by a factor $7.8\Delta v_5 T_{c10}^{-1/2}$, lowering the equilibrium temperature for a given flux and shifting more of the power into lower lying rotational lines.

2.3.3. *Gas-Grain Cooling*

Since grains embedded in cooling-flow clouds remain relatively cold, they can assist in cooling the gas. Gas-grain interactions cool molecular gas of pressure $n_{H_2} T = 3 \times 10^5$ cm^{-3} K at the rate

$$(2.3 \times 10^{-27} \text{ ergs s}^{-1}) \left(1 - \frac{T_{d10}}{T_{c10}}\right) \chi_d T_{c10}^{1/2}$$

per H nucleus, where T_{d10} is the dust temperature in units of 10 K (Hollenbach & McKee 1989). If radiative heating cannot raise the grain temperature above the gas temperature, dust converts thermal energy into infrared photons.

Optical/UV radiation from galaxies in the cluster core impinges on dust at 100 kpc radius with a flux $\sim 10^{-3}$–10^{-4} ergs cm^{-2} s^{-1}. Grains at ~ 10 K absorb this radiation with an efficiency $Q_{abs} \sim (1\text{–}10)a_\mu$, where a_μ is the grain radius in microns, and reradiate the incident flux in the far-infrared with a Planck-averaged efficiency $\sim 10^{-3} a_\mu$ (Draine & Lee 1984). Stellar radiation thus heats intracluster dust to 6–20 K. Deeper than $N_H \sim 10^{21}$ cm^{-2} into a cloud with $\chi_d \sim 1$, extinction reduces this radiative heating.

Gas-grain cooling can be important only in cooling-flow clouds colder than 20 K and thicker than 10^{21} cm^{-2}. Because dusty clouds remain optically thin in the far-infrared to very large column depths, gas-grain cooling is not blackbody-limited like molecular line cooling. However, reradiating an absorbed X-ray flux of $\sim(10^{-5}$ ergs cm^{-2} s$^{-1})F_5$ via dust emission requires a cloud thicker than

$$(4.4 \times 10^{22} \text{ cm}^{-2}) \left(1 - \frac{T_{d10}}{T_{c10}}\right)^{-1} \chi_d^{-1} T_{c10}^{-1/2} F_5 .$$

Such a cloud with $T_{d10} \ll T_{c10} \sim 1$ would produce $\sim 3F_5$ mag of optical extinction.

2.4. *Thermal Structure*

In a steady state, heating balances cooling. When the optical depths of the major cooling transitions are less than n_{cr}/n_H,

radiative trapping is not important, and equating the heating and cooling rates per unit volume at each depth sets the equilibrium temperature. At higher optical depths, thermalization of the major lines allows photons generated at one depth to heat gas at another depth. Radiation thermally couples these regions, and balance between heat flux in and cooling flux out determines the equilibrium temperature, which does not vary much with depth.

2.4.1. *Neutral Atomic Gas*

Equating the X-ray heating rate for atomic gas ($H_{\rm heat,H\,I}$) and the sum of the optically thin fine-structure line cooling rates for FFJ abundances gives the equilibrium temperatures pictured in Figure 3. Although this calculation is crude, it predicts a thermal structure that differs only modestly from that calculated by FFJ from $N_{\rm H} \sim 10^{19}$ cm^{-2} to beyond 10^{21} cm^{-2}. However, deeper than $N_{\rm H} \sim 10^{20}$ cm^{-2}, the [C I] fine-structure lines should thermalize, and local thermal balance no longer applies. From this depth to $N_{\rm H} = (10^{21}\ {\rm cm}^{-2})N_{21}$, the integrated X-ray heating flux (§ 2.1) is

$$(1.1 \times 10^{-6}\ {\rm ergs\ cm^{-2}\ s^{-1}})(1 - f_g)\dot{M}_{100} r_{100}^{-2} \ln(10 N_{21}) .$$

Setting $N_{21} = \dot{M}_{100} = r_{100} = 1$ and $f_g \ll 1$ gives a fiducial heating flux $F_{\rm at} \equiv 2.6 \times 10^{-6}$ ergs cm^{-2} s^{-1}. Figure 4 compares this fiducial flux, plus fluxes 3 times greater and smaller, with optically thick line cooling fluxes from C I and O I, assuming their line widths are thermal. Deep inside fully atomic clouds, gas temperatures cannot fall much below 10 K, unless turbulence broadens the cooling lines, enabling more flux to escape without violating the blackbody limit. Gas temperatures inside static atomic cooling-flow clouds should level off between 10 and 20 K.

2.4.2. *Neutral Molecular Gas*

The most important rotational lines of CO become optically thick and thermalized at $N_{\rm H} \sim 10^{19}$ cm^{-2} in a molecular cooling-flow cloud of near solar abundances. From here to depth $N_{21}(10^{21}\ {\rm cm}^{-2})$, X-rays deposit a total heat flux (§ 2.1)

$$(2.9 \times 10^{-6}\ {\rm ergs\ cm^{-2}\ s^{-1}})(1 - f_g)\dot{M}_{100} r_{100}^{-2} \ln(100 N_{21}) .$$

Figure 2 illustrates how the fiducial heating flux $F_{\rm mol} \equiv 1.3 \times 10^{-5}$ ergs cm^{-2} s^{-1} and fluxes 3 and $\frac{1}{3}$ times $F_{\rm mol}$ relate to the various molecular line cooling fluxes discussed earlier. The resulting range of equilibrium temperatures runs from 25 to 51 K for the Goldsmith & Langer (1978) cooling function and from 16 to 30 K for the Hollenbach & McKee (1979) cooling function. Even in the extreme limit where all the CO lines are thermalized, the equilibrium temperature stays above 10 K. Turbulence that increases the line widths over their thermal values can lower the equilibrium temperature by boosting the CO 1–0 and 2–1 fluxes.

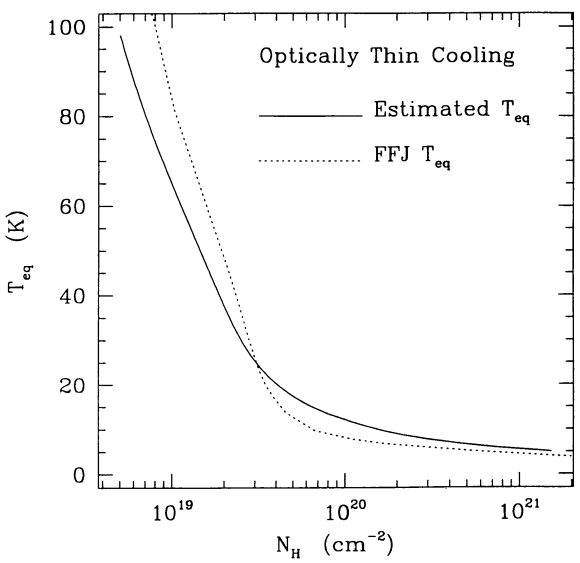

FIG. 3.—Equilibrium temperatures in optically thin atomic cooling-flow clouds. Solid line traces the equilibrium temperature $T_{\rm eq}$ as a function of $N_{\rm H}$ in an atomic cooling-flow cloud with FFJ abundances. Equating the estimated heating rate $H_{\rm heat,H^0} = (1.1 \times 10^{-27}\ {\rm ergs\ s^{-1}})(N_{\rm H}/10^{21}\ {\rm cm^{-2}})^{-1}$ and the cooling function from Fig. 1 for $n_{\rm H}\,T = 2.9 \times 10^5$ cm^{-3} K sets $T_{\rm eq}$. Dotted line shows the function $T_{\rm eq}(N_{\rm H})$ from FFJ.

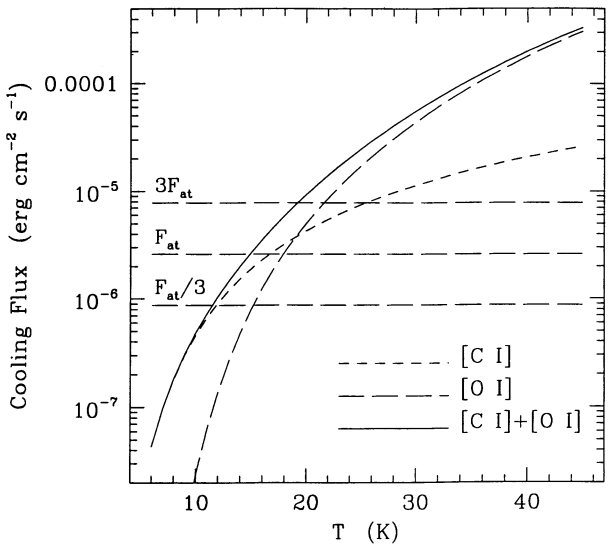

FIG. 4.—Optically thick atomic line cooling. The atomic fine-structure line fluxes from a cloud in which the [O I] 63 μm and 145 μm lines and the [C I] 370 μm and 610 μm lines have all become optically thick are shown.The line widths are assumed to be $\Delta v_{\rm FWHM} = 2.355(kT_{\rm cl}/A_Z m_{\rm H})^{1/2}$, where A_Z is the atomic weight. Dotted lines show the range of X-ray heating fluxes expected in atomic cooling flow clouds. Temperatures inside atomic cooling-flow clouds with thermal line widths fall into the range 10 to 20 K and cannot drop much below 10 K unless the lines are turbulently broadened.

2.5. *Contrasts between Previous Models*

Current H I 21 cm and CO 1–0 line observations strongly constrain the covering factors of cooling-flow clouds if their temperatures are 20 K or greater but do not impose such stringent limits if cloud temperatures are close to the microwave background temperature. Although the models of FFJ and Fabian et al. (1994) predict that cooling-flow cloud temperatures can drop below 4 K, calculations of thermal balance in molecular cooling-flow clouds by OBMTS find equilibrium temperatures an order of magnitude higher. Here we discuss why these two temperature estimates disagree.

Unlike FFJ, the OBMTS calculation considers cooling-flow clouds that are molecular and, by implication, dusty. When X-rays are absorbed, OBMTS assume 50% of their energy converts into heat. The actual conversion efficiency should be somewhat lower. Up to half of the X-ray energy could go directly into grain heating (§ 2.1), and Glassgold & Langer (1973) find that only one-third of the remainder ends up as heat. In a 6 keV ICM with $n_{\rm H} = 2 \times 10^{-3}$ cm^{-3} at 100 kpc, OBMTS find a heating rate $\sim 3 \times 10^{-27}$ ergs s^{-1} per H

nucleus at $N_H = 10^{21}$ cm^{-2}, similar to the rate found in § 2.1, except for the factor $1 - f_g$. Equating X-ray heating at this depth with the cooling functions of Goldsmith & Langer (1978), OBMTS find equilibrium temperatures of 20–40 K, in agreement with those determined in Figure 2. Since small changes in temperature produce large changes in the molecular cooling rate, modest inaccuracies in X-ray heating efficiencies do not alter equilibrium temperatures significantly.

In the models of FFJ, dust-free gas remains primarily atomic to $N_H = 4 \times 10^{21}$ cm^{-2}, so FFJ use the analytic fit of Shull & Van Steenberg (1985) to compute the X-ray heating efficiency. This formula is valid for $X_e \geq 10^{-4}$, the lowest fractional ionization considered by Shull & Van Steenberg (1985), but drops to zero as $X_e \rightarrow 0$, whereas the actual heating efficiency should remain near 10% (Xu & McCray 1991). The FFJ model therefore underestimates the heating rate by a factor of 2 to 3 at high N_H, at which $X_e \sim 10^{-6}$. Equilibrium temperatures determined by FFJ are similar to those we estimate when assuming optically thin cooling and are even lower at high N_H, reflecting this underestimate of the heating rate. However, line cooling at high N_H in cooling-flow clouds should not be optically thin, and optically thick cooling predicts equilibrium temperatures no lower than 10 K (Fig. 4).

Dusty cooling-flow clouds, modeled by Fabian et al. (1994), become fully molecular at columns less than 10^{20} cm^{-2}, depending on the dust-to-gas ratio. It is not clear whether these models include dissociative recombination of H_2^+ via H_3^+ as a heat source. When carbon becomes fully molecular, equilibrium temperatures plunge to $\sim$3 K. At this point ($N_H \sim 10^{20}$ cm^{-2}) the models terminate without considering how energy deposited into deeper layers escapes. In these clouds, the CO lines should be optically thick, and Figure 2 shows that the equilibrium temperatures of such clouds should remain above 10 K, even if the clouds convert only 1% of the incident X-ray flux into heat.

The FFJ and Fabian et al. (1994) models use escape probability techniques to account for radiative trapping, but deep inside cooling-flow clouds, the assumptions underlying these techniques break down. Escape probability computations of optically thick cooling rates presume that the source function, and therefore the excitation temperature, is constant throughout the optically thick region. At the densities of cooling-flow clouds, the [C I] and low-lying CO lines are thermalized, so the excitation temperature equals the gas temperature. FFJ and Fabian et al. (1994) balance local heating and locally determined optically thick cooling to find the equilibrium gas temperature at a given depth. Their results show that the local heating rate drops quickly enough with increasing N_H to produce a significant temperature gradient across the optically thick zone, violating the assumption of a constant source function. If the source function decreases into the cloud, photons will diffuse from the cloud's warmer layers into the cooler interior, providing heating not accounted for in the escape probability treatment. Furthermore, since the line widths in the cool inner region are significantly narrower than those further out, the escape probability formalism severely overestimates the odds that a photon produced near the cloud's center will escape. If line widths throughout a cooling-flow cloud are thermal and all the important cooling transitions are optically thick, dT_{cl}/dN_H will be positive in an optically thick zone in which heating and cooling balance. Since X-ray heating drops rapidly with depth, this gradient need not be very large, so the constant temperature and global flux balance assumptions provide good estimates of equilibrium temperature. Thus, cooling-flow cloud temperatures should be near 20 K, as predicted by OBMTS, and such clouds should be detectable.

3. LIMITS ON ATOMIC GAS

The deepest searches for H I in cooling-flow clusters usually take advantage of the Arecibo telescope's enormous collecting area and appropriate beam size of 3.3 at 21 cm. Arecibo observations show that nearby clusters contain no more than 10^9–10^{10} $M_\odot$ of optically thin H I (e.g., McNamara, Bregman, & O'Connell 1990), but the amount of optically thick H I can be much larger if cooling-flow clouds are cold. These measurements can also be used to limit the covering factors of atomic gas within the cooling radii of these clusters. The expected signal is the product of the total 21 cm flux from the surface of an atomic cooling-flow cloud and the beam covering factor. At the distances of nearby cooling-flow clusters ($z \sim 0.01$–0.06), the Arecibo beam subtends an area with a radius less than 200 kpc, so the beam covering factor (f_{HI}) and the covering factor of X-ray–absorbing clouds (f_X) in the cooling flow should be about the same. Since temperatures deep within X-ray–irradiated cooling-flow clouds are well regulated, 21 cm flux limits impose strong upper limits on f_{HI}. This section shows that $f_{HI} < 0.1$.

3.1. *Theoretical Expectations*

The brightness temperature in the core of an optically thick 21 cm line from a cloud at typical interstellar densities equals the gas temperature at which the line becomes opaque. Atomic cooling-flow clouds have dropped to $\sim$20 K at $N_H \approx 4 \times 10^{19}$ cm^{-2}, and the 21 cm optical depth of a homogeneous H I cloud with thermal line widths reaches unity at $N_H = (1.5 \times 10^{19}$ cm$^{-2})T_{c10}^{3/2}$. H I lines from such clouds therefore have characteristic temperatures of 20 K in both emission and absorption. Integrating the 21 cm transfer equation over the FFJ relation for $N_H(T)$, we obtain a total 21 cm line flux of 24.5 K km s^{-1} over a baseline temperature of 2.735 K. If the baseline temperature is $\gg$20 K, the 21 cm line from an FFJ cloud has an absorption equivalent width of 1.2 km s^{-1}. Turbulent line widths increase both the integrated line flux and the absorption equivalent width.

In a large beam, the detectability of emission or absorption features depends on $\mathcal{N}_{HI}$, the average number of optically thick H I clouds along a line of sight through the cooling flow. Since two superposed clouds are unlikely to cover each other in velocity space, the integrated line flux or equivalent width equals the flux or width per cloud times $\mathcal{N}_{HI}$. Atomic clouds can produce the observed X-ray absorption only if $f_{HI} \sim 1$, implying $\mathcal{N}_{HI} \gtrsim 1$.

3.2. *Observational Limits*

McNamara et al. (1990) observed 11 nearby cooling-flow clusters from Arecibo without detecting H I 21 cm emission. The typical rms noise in each 9 km s^{-1} channel was $\lesssim$1 mJy in flux, corresponding to $\lesssim$8 mK in brightness temperature. Over a line width of (300 km s^{-1})v_{300}, the 3 σ limit on the beam-averaged 21 cm brightness is less than (1.25 K km s^{-1})$v_{300}^{1/2}\,\sigma_{mJy}$, where σ_{mJy} is the rms noise in millijanskys. This limit implies $\mathcal{N}_{HI} < 0.05 v_{300}^{1/2}\,\sigma_{mJy}$. Other Arecibo emission-line observations (Burns, White, & Haynes 1981; Valentijn & Giovanelli 1982) yield similar limits, and 21 cm absorption-line studies find $f_{HI} \lesssim 0.2$ (Jaffe 1992; O'Dea, Gallimore, & Baum 1995). A recent VLA study of three clusters also limits optically

thin H I masses to less than $10^{9-10}\ M_\odot$ and finds $f_{\rm H\,I} < 0.36$ (Dwarakanath, van Gorkom, & Owen 1994).

Because of uncertainties in determining the instrumental baseline structure over the effective bandwidth of $\sim$2000 km s^{-1}, the emission-line limits derived from MBO are valid only up to $v_{300} \sim 3$ (B. McNamara, private communication). The velocity dispersions of nearby cooling-flow clusters (500–800 km s^{-1}) correspond to full line widths $\sim$1200–1900 km s^{-1}, but clouds at these speeds would be moving transonically through the intracluster medium. In $\sim 10^8$ yr, ICM drag slows clouds of $N_{\rm H} \sim 10^{21}$ cm^{-2} to speeds similar to turbulent velocities in the ICM. Daines et al. (1994) argue that since the H I line width in the E0 galaxy M86 implies motions with a Mach number of 0.4 (Bregman & Roberts 1990), intracluster turbulence might produce H I line widths $\sim$500–800 km s^{-1}. The MBO bandwidth of $\sim$2000 km s^{-1} suffices for lines this wide, contrary to the claim in Daines et al. that MBO could detect only lines narrower than $\sim$400 km s^{-1}. Limits on $f_{\rm H\,I}$ imposed by the MBO data are therefore much more stringent than those given by Daines et al. (1994). Figure 5 displays the 3 σ limit on $\mathcal{N}_{\rm H\,I}$ and the projected radius of the Arecibo beam (r_b) for each cluster, assuming a Hubble constant of 75 km s^{-1} Mpc^{-1}.

To rule out extraordinarily wide emission lines from clusters, O'Dea & Payne (1991, 1995) have observed 14 clusters at Arecibo with a bandwidth of 7000 km s^{-1}. They detect nothing at rms noise levels as low as 0.2 mJy (for A2063). The expected flux density is (10 mJy)$\mathcal{N}_{\rm H\,I} v_{300}^{-1}$. Even if the H I full width is 2000 km s^{-1}, these observations rule out $f_{\rm H\,I} > 0.3$ at the 3 σ level.

3.3. *Dust Requirements*

The 21 cm limits imply that cold clouds cannot cover cooling flows unless hydrogen forms molecules at $N_{\rm H} \ll 4 \times 10^{19}$ cm^{-2}. If $f_X \sim 1$ in cold clouds, the average column density of H I across the Arecibo beam must be $\lesssim 4 \times 10^{18}$ cm^{-2}. Molecule formation rapid enough to turn a cooling-flow cloud molecular at this small a depth requires a nearly Galactic dust-to-gas ratio (see § 2.2.1). Hydrogen in the dusty cooling-flow clouds ($\chi_d = 1$) modeled by Fabian et al. (1994) goes from atomic to molecular at $N_{\rm H} \approx 2 \times 10^{18}$ cm^{-2}. Carbon in these clouds goes entirely into CO at $N_{\rm H} \approx 3 \times 10^{19}$ cm^{-2}. The next section shows that CO flux limits constrain the covering factors of molecular cooling-flow clouds also to be $\ll 1$.

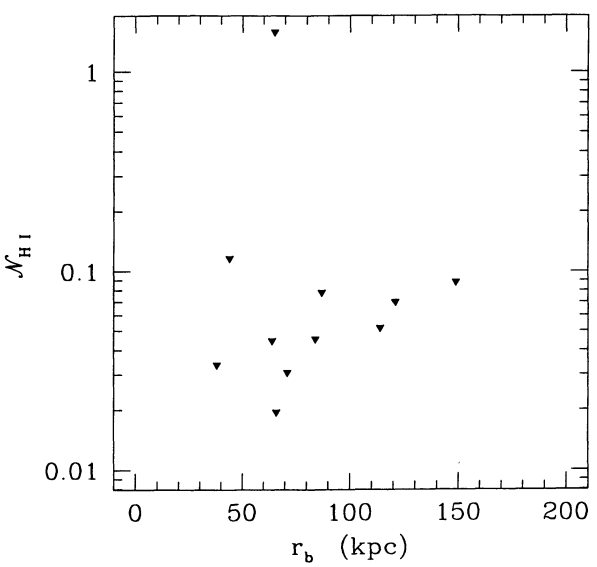

FIG. 5.—Limits on H I clouds. The 3 σ limits on the average number of atomic clouds $\mathcal{N}_{\rm H\,I}$ along lines of sight through cooling flows derived from the Arecibo observations of MBO are shown. The quantity r_b is the projected half-power radius of the Arecibo beam at the distances of these clusters, assuming $H_0 = 75$ km s^{-1} Mpc^{-1}.

4. LIMITS ON MOLECULAR GAS

None of the recent high-sensitivity searches for CO rotational lines from the centers of cooling-flow clusters other than the Perseus cluster have detected strong emission (Bregman & Hogg 1988; Grabelsky & Ulmer 1990; OBMTS; McNamara & Jaffe 1994; Braine & Dupraz 1994; Antonucci & Barvainis 1994). Applying the usual Galactic CO luminosity to H_2 mass conversion factor to these nondetections constrains the H_2 masses at the centers of these clusters to be less than 10^8–10^{10} $M_\odot$, but this conversion factor is not necessarily universal (e.g., Maloney & Black 1988). Processes that heat and disturb Galactic molecular clouds, like star formation, magnetohydrodynamic wave dissipation, and cosmic-ray ionization, might not operate in intracluster molecular clouds. However, X-ray heating sufficient to keep cloud temperatures above 10 K is unavoidable (§ 2.4.2; see also Braine et al. 1995). This section compares the minimum integrated brightnesses of CO lines expected from molecular cooling-flow clouds with the observational limits. We find that the average number of molecular clouds ($\mathcal{N}_{\rm H_2}$) along a line of sight through a cooling flow is significantly less than unity. We also show that X-rays inhibit condensation of CO onto dust grains, so that the low-lying CO lines remain optically thick and strongly emitting.

4.1. *Theoretical Expectations*

The CO observations mentioned above have beam sizes ($<1'$) that fall well within the cooling radii of nearby clusters. The value of $1 - e^{-\mathcal{N}_{\rm H_2}}$ in the beam is therefore a good measure of the molecular cloud contribution to f_X. Assuming that line widths are thermal minimizes the CO 1–0 and 2–1 line fluxes expected from molecular cooling-flow clouds, which must then be at about 20 K (§ 2.4.2). Because the total flux radiated by a cooling-flow cloud flux must balance the absorbed flux, turbulent broadening *increases* the integrated CO 1–0 line flux from a cooling flow cloud, even though it lowers the brightness temperature in the line core.

The integrated brightness of a thermalized, thermally broadened CO line is $2(2kT_{\rm cl}/28m_{\rm H})^{1/2} T_{\rm cl} F_{\rm sat}(\tau_0)$, where $F_{\rm sat}$ is a saturation factor that depends on the line center optical depth τ_0. When $\tau_0 \gg 1$, $F_{\rm sat}(\tau_0) \approx (\ln \tau_0)^{1/2}$ (Spitzer 1978). In LTE at 20 K, about 13% of the CO molecules have $J = 0$. Thus, the line center $J = 1$–0 optical depth is $\sim 10^2$ in a cloud with $N_{\rm H} \sim 10^{21}$ cm^{-2} and a solar abundance of C in CO. Setting $F_{\rm sat} \approx 2$ and $T_{\rm cl} = 20$ K, we find an intensity of $\sim$9 K km s^{-1} for each optically thick CO line from the surface of an individual cloud. The expected beam-averaged signal is $\mathcal{N}_{\rm H_2}$ times this amount.

4.2. *Observational Limits*

Recent CO observations of clusters probe down to rms noise levels of a few mK, imposing 3 σ limits <1 K km s^{-1} on the integrated CO brightnesses of clusters. McNamara & Jaffe (1994) looked for CO $J = 2$–1 emission in six clusters and obtained 3 σ intensity limits of less than 0.419–0.989 K km s^{-1}, assuming a line width $v_{300} = 1$ inside their 680 km s^{-1} band.

Braine & Dupraz (1994) observed eight clusters in $J = 2$–1 (665 km s^{-1} bandwidth) and $J = 1$– 0 (1330 km s^{-1} bandwidth). Assuming $v_{300} = 1$, they obtained 3 σ limits of <0.24–1.05 K km s^{-1} for $J = 2$– 1 and of <0.39–0.66 K km s^{-1} for $J = 1$–0. The larger bandwidth in $J = 1$–0 constrains lines with $v_{300} = 2$ to be less than <0.65–1.09 K km s^{-1}. Bregman & Hogg (1988) and Grabelsky & Ulmer (1990) limit the CO 1–0 intensity to similar levels over a similar bandwidth in 11 clusters, some of which are in the Braine & Dupraz (1994) sample, and OBMTS limit the 1–0 line emission from three more clusters to levels about the same as those in the other surveys. Figure 6 shows the upper limits from the four surveys for intracluster CO $J = 1$–0.

Since the integrated CO brightnesses of these objects are consistently less than 1 K km s^{-1} for line widths $\lesssim 600$ km s^{-1}, the molecular covering factor must be $f_{H_2} < 0.1$. Molecular line widths in clusters are unlikely to be much larger than 600 km s^{-1} (see § 3.2). In NGC 1275 at the center of the Perseus cluster, where intracluster CO has been detected (Lazareff et al. 1989; Mirabel et al. 1989; Braine et al. 1995), its line width (<400 km s^{-1}) is much thinner than the bandwidth observed. To rule out very broad lines observationally, Antonucci & Barvainis (1994) have constrained the brightnesses of emission lines with widths of up to 2500 km s^{-1} in five clusters. Their 3 σ limits on the brightness temperature of CO 1–0 at line center over the baseline established at ± 1300–2000 km s^{-1} are ~ 9 mK and rule out $\mathcal{N}_{H_2} = 1$ for line widths of 1000 km s^{-1}. One of the objects in their sample is A478, the same cluster in which Allen et al. (1993) found very strong soft X-ray absorption.

4.3. *Condensation of CO onto Dust*

Fabian et al. (1994) have suggested that cooling-flow clouds might be so cold, quiescent, and long-lived that all the CO condenses onto grains. If molecular cooling-flow clouds with $f_{H_2} \sim 1$ are to evade current observational limits, condensation of CO would have to be quite complete. The $J = 1$–0 transition in our standard cooling-flow clouds will not become optically thin unless the fraction of CO in the gas phase drops below 10^{-2}. If all the metal-bearing molecules condense onto grains, the only coolants left are H_2, He, or grains. X-ray heating via photoionization of H_2 and He would then raise the gas temperature until heating is balanced by gas-grain cooling or H_2 line emission. However, condensation of molecules onto grains is unlikely to be so complete. Transient heating of grains and grain surfaces by X-rays in cooling-flow clouds unbinds CO from grain surfaces much more rapidly than cosmic-ray heating of grains in Galactic molecular clouds, in which gas-phase CO is abundant. The following paragraphs evaluate X-ray transient heating of grains to estimate CO desorption rates in cooling-flow clouds and show that X-ray desorption operates faster than condensation, keeping the CO in the gas phase.

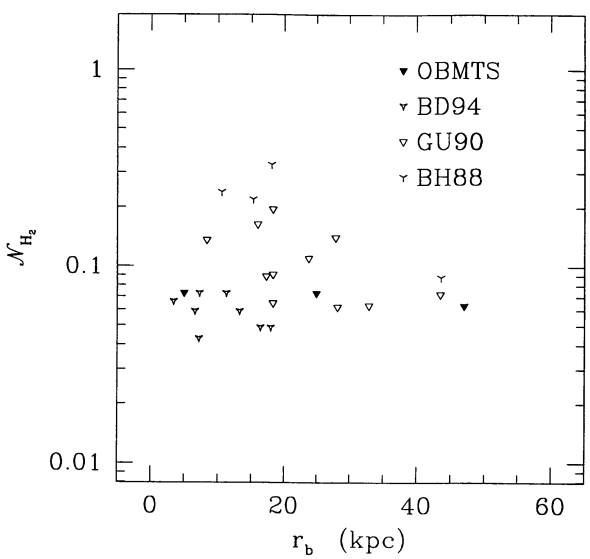

FIG. 6.—Limits on H_2 clouds. The 3 σ limits on the average number of molecular clouds $\mathcal{N}_{H_2}$ along lines of sight through cooling flows are shown. These limits were derived from CO $J = 1$–0 intensity limits, assuming cloud temperatures of 20 K, thermal line widths, highly optically thick CO 1–0 lines, and overall line widths of 600 km s^{-1}. Symbols denote upper limits calculated from the data of Braine & Dupraz (1994) (BD94), Grabelsky & Ulmer (1990) (GU90), Bregman & Hogg (1988) (BH88), and OBMTS. The quantity r_b is the projected half-power radius of each beam at the distances of the clusters, assuming $H_0 = 75$ km s^{-1} Mpc^{-1}.

4.3.1. *Condensation Rates*

Carbon monoxide molecules in molecular clouds at a pressure of 3×10^5 K cm^{-3} encounter a dust grain within $\sim(2 \times 10^{12}$ s$)\chi_d^{-1} T_{c10}^{1/2}$. Let us assume that CO molecules always stick when they collide with a grain. Then CO in molecular cooling-flow clouds can potentially condense onto dust grains in $\sim 10^5$ yr. If there is a solar abundance of carbon in CO, the flux of CO molecules impinging on a grain surface is $\sim(5 \times 10^4$ cm^{-2} s$^{-1})T_{c10}^{-1/2}$. Dust grains a_μ microns in size therefore grow on a timescale $\sim(7 \times 10^{13}$ s$)T_{c10}^{1/2} a_\mu$.

4.3.2. *X-Ray Transient Heating*

Photons in the 1 keV range impinge on grains in cooling-flow clouds with a flux $\sim(1.4 \times 10^4$ cm^{-2} s$^{-1})\dot{M}_{100} r_{100}^{-2}$. Not all are absorbed. Since 1 μm grains are marginally optically thick at 1 keV, smaller grains absorb photons of this energy about once every $\sim(2 \times 10^3$ s$)\dot{M}_{100}^{-1} r_{100}^2 a_\mu^{-3}$. Between X-ray absorption events, accretion of CO onto small grains increases their X-ray cross sections. The maximum time between X-ray captures is $\sim(2 \times 10^{11}$ s$)\dot{M}_{100}^{-1} r_{100}^2$, by which time even the smallest grains have grown to ~ 0.002 μm.

As grains smaller than 0.05 μm absorb X-rays, their temperatures temporarily rise above 25 K (Leger, Jura, & Omont 1985, hereafter LJO; Voit 1991b). At these temperatures, grains with CO mantles cool primarily by shedding CO molecules. Since the binding energy of CO onto grains is ~ 0.1 eV (LJO), a keV photon can expel $\sim 10^4$ CO molecules from a single grain. Averaged over time, transient heating induces an evaporative CO flux from the grain surface $\sim(4 \times 10^7$ cm^{-2} s$^{-1})\dot{M}_{100} r_{100}^{-2} a_\mu^{-1}$. This flux exceeds the condensing flux even at the minimum radius of 0.002 μm. Chemical explosions ignited in the CO mantle when the grain temperature rises above 27 K can raise the evaporative flux even further (LJO). Transient heating thus prohibits substantial CO depletion onto small grains in cooling-flow clouds.

4.3.3. *X-Ray Spot Heating*

Although X-ray impacts do not alter the global temperatures of large grains (>0.1 μm) appreciably, small regions surrounding the sites of X-ray absorption briefly become warm enough to unbind CO before the photon's heat input diffuses throughout the rest of the grain. Capture of 1 keV photon within a grain releases two or more sub-keV electrons. These electrons deposit ~ 35–60 keV μm^{-1} into heat before they either stop within the grain or escape from its surface (LJO;

Dwek & Smith, private communication quoted in Voit 1991b). A 500 eV electron travels ~ 0.01 μm before it stops. The temperature of the heated cylinder surrounding the electron's path declines as the heat diffuses outward. Following the analysis of cosmic-ray spot heating by LJO, we assume that the radius of this hot cylinder expands as $r_{\rm cyl} \approx 1.7\alpha_d t_d$, where $\alpha_d = 1.1 \times 10^{-2}$ cm^2 s^{-1} is the thermal diffusivity and t_d is the time since the heating event. Given a heat capacity of $(2.2 \times 10^4$ ergs cm^{-3} K$^{-2.3})T_{\rm cyl}^{1.3}$ for grain material at temperature 50 K $< T_{\rm cyl} < 150$ K (LJO), we find $T_{\rm cyl} \sim 120 t_{11}^{-0.43}$, where $t_{11} = t_d/10^{11}$ s.

Molecules within the disks at which hot cylinders intersect the grain surface evaporate as long as the evaporation rate exceeds the diffusion rate. Carbon monoxide molecules evaporate on a timescale of $\sim(1.4 \times 10^{-15}$ s) exp (1030 K$/T_{\rm cyl})$ (LJO), so evaporation proceeds until $t_{11} \gtrsim 1$, when $r_{\rm cyl} \sim 60$ Å. As the grain cools evaporatively, thermal energy diffuses toward the grain surface as well as away from the electron's path. If CO molecules cover the grain surface, a disk 60 Å in radius encompasses $\sim 10^4$ molecules. The available thermal energy (~ 500 eV) can unbind only about half of these molecules, so evaporative cooling halts CO desorption before thermal diffusion does.

Each keV X-ray absorbed within ~ 0.01 μm of the surface of a large grain produces, on average, one hot cylinder that intersects the grain surface. If CO molecules cover the grain, each X-ray absorption in this surface layer releases 10^3 or more CO molecules. Since the 1 keV optical depth of this layer is $\sim 10^{-2}$, the induced evaporative flux of CO from the grain surface is $\gtrsim(1.4 \times 10^5$ cm^{-2} s$^{-1})\dot{M}_{100} r_{100}^{-2}$. This is sufficient to keep most of the CO in the gas phase and rules out the nearly complete condensation needed to render the CO rotational lines optically thin. This should not be surprising. Evaporation through X-ray spot heating in cooling-flow clouds is 3 orders of magnitude faster than the cosmic-ray spot heating thought to keep CO in the gas phase in Galactic molecular clouds (LJO).

5. DUST IN THE HOT GAS

The previous two sections have shown that atomic or molecular clouds that cover the cooling-flow regions of clusters should already have been detected. If X-ray self-absorption in clusters is real, then either (1) the X-ray absorption comes from ionized gas, (2) the X-ray absorption comes from solid state particles in the hot medium, or (3) the X-ray emission comes from unresolved filaments of low covering factor spatially correlated with clouds of cool absorbing gas (Antonucci & Barvainis 1994). In this section we examine options (1) and (2). We rule out ionized gas because it would be emitting optical, UV, or X-ray lines profusely, and these lines are not seen. The second option is more difficult to dismiss. The amount of dust needed to make the ICM marginally optically thick in soft X-rays would also make it marginally optically thick in the optical band. We discuss how the required extinction might be consistent with surveys that find a deficit of background objects behind clusters, and we show that far-IR flux limits prohibit the absorbing dust from being in the central parts of the cluster.

5.1. *Hot Gas Only*

Gas cool enough for oxygen K-shell electrons to remain bound can absorb soft X-rays. In coronal ionization equilibrium, the fraction of oxygen nuclei with bound electrons drops off rapidly above 3×10^6 K (e.g., Shull & Van Steenberg 1982). When $T < 3 \times 10^6$ K, CNO nuclei retain one or more electrons, and radiative cooling is very efficient. At cooling-flow pressures, the luminosity radiated by ionized absorbing gas would be orders of magnitude higher than that from the cooling flow, making it very unlikely, on theoretical grounds, that the absorbing gas is ionized. To eliminate this possibility observationally, we have calculated the expected surface brightnesses of several emission lines at various temperatures, assuming an absorbing column of 10^{21} cm^{-2}. Comparing these expectations with the Hα and [Fe x] 6374 Å limits from deep Palomar long-slit spectra, we can rule out ionized absorbing gas at temperatures less than 1.5×10^6 K in several clusters. At higher temperatures, an enormous O VIII Lyα luminosity should have been detected but is not.

5.1.1. *Line Emission from Ionized Gas*

We have used the code CLOUDY 84.12a (Ferland 1993) to calculate cooling functions (in ergs cm^3 s^{-1}) for individual lines emitted by a solar abundance plasma in coronal equilibrium at temperature T. Multiplying these cooling functions by the density $(3 \times 10^5$ K cm$^{-3})T^{-1}$ and the column density 10^{21} cm^{-2} and then dividing by 4π sr gives the expected surface brightnesses of these lines, pictured in Figure 7. On the right side of Figure 7 we show the corresponding luminosities, assuming an emitting area of $\pi(100$ kpc$)^2$. When 10^5 K $< T < 10^6$ K, the UV emission lines are extremely luminous. Pistinner & Sarazin (1994) have compiled a large list of UV line brightnesses expected from ionized absorbing gas in cooling flows. Observations with the *Hubble Space Telescope*, the *International Ultraviolet Explorer*, the *Hopkins Ultraviolet Telescope* can potentially constrain ionized absorbing columns

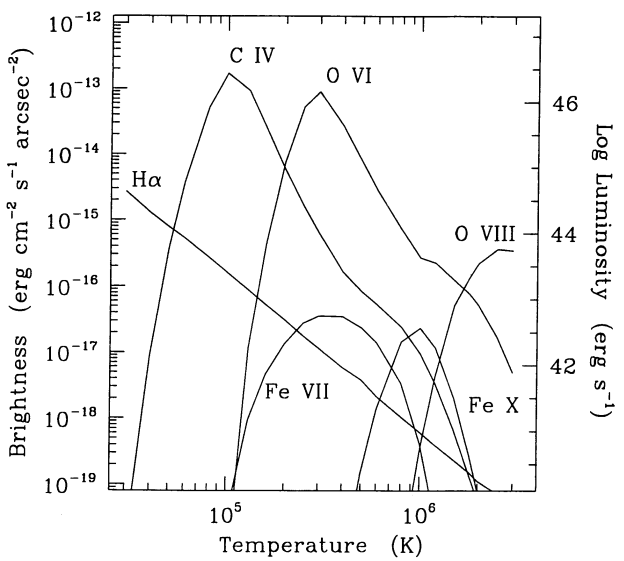

FIG. 7.—Surface brightnesses of absorbing H II gas. A 10^{21} cm^{-2} column of ionized gas at the pressure of the cooling flow shines brightly in emission lines. The variation of surface brightnesses of selected lines with temperature is illustrated, assuming $N_{21} = 1$, solar metallicity, and coronal ionization equilibrium at a pressure of 3×10^5 K cm^{-3}. Cooling functions for the following lines were calculated using CLOUDY 84.12a (Ferland 1993): Hα, C IV 1550 Å, O VI 1036 Å, O VIII Lyα at 653 eV, [Fe VII] 6087 Å, and [Fe X] 6374 Å. Our long-slit spectroscopic limits on Hα and [Fe X] rule out $N_{21} \gtrsim 1$ in ionized gas at temperatures below 1.5×10^6 K. Along the right axis we show line luminosities, assuming $N_{21} \sim 1$ over a radius of 100 kpc. O VIII Lyα luminosities of greater than 10^{43} ergs s^{-1} are not seen, ruling out higher temperature gas.

at these temperatures. When 1.5×10^6 K $< T < 3 \times 10^6$ K, the O VIII Lyα luminosity from the central 100 kpc exceeds 10^{43} ergs s^{-1}. The equivalent width of this line with respect to the underlying cooling-flow spectrum from § 2.1 is $\sim$250 eV. Such strong O VIII lines have not been seen in ASCA spectra of cooling-flow clusters (Fabian et al. 1994).

5.1.2. *Optical Spectroscopic Limits*

Ionized X-ray absorbing gas at $T < 1.5 \times 10^6$ K can be ruled out in several cooling-flow clusters for which we have deep ground-based spectroscopic observations. The Palomar and Las Campanas long-slit observations described in Donahue & Stocke (1994) tightly constrain the off-nuclear surface brightnesses of Hα and [Fe X] 6374 Å in A1795, 2A0335+096, and PKS 0745−191. We report these limits here. The data comprise a subset of the original observations (A1795, 4500 s at PA 345 on 1992 December 31; 2A0335+096, 8100 s at PA 140 on 1992 December 31; PKS 0745−191, 8400 s at PA 235 and 3000 s at PA 180 on 1992 December 19). We analyzed the residual sky spectra, summed in 10″ bins along a 2″ slit, in the sky-subtracted, flux-calibrated images. We converted the rms variation of the residual sky ($\sigma_{\rm rms}$ in erg s^{-1} cm^{-2} Å^{-1}) near the redshifted wavelengths of Hα and [Fe X] into a 3 σ surface brightness limit equal to

$$\frac{3\sigma_{\rm rms}(10\ \text{Å}/d)^{1/2}}{20\ \text{arcsec}^2}, \tag{8}$$

where d is the dispersion of the spectrograph in units of Å per pixel.

The 3 σ surface brightness limits on both Hα and [Fe X] away from the emission-line nebulae in these clusters are <2–4×10^{-18} ergs s^{-1} cm^{-2} arcsec^{-1} (see Table 1). Because these limits are derived from sky-subtracted images, they do not constrain an absolutely smooth and uniform distribution of emission-line surface brightness. However, since absorbing gas at intermediate temperatures must have a small filling factor, its distribution ought to be clumpy rather than smooth. These limits on the brightnesses of Hα and [Fe X] constrain the column density of ionized X-ray absorbing gas at $T < 1.5 \times 10^6$ K to be less than 10^{21} cm^{-2}.

The faintest detected nebular surface brightnesses in A1795 and 2A0335+096 are consistent with our upper limits farther off nucleus. In A1795, where the slit was aligned along the extended nebula, the Hα surface brightness drops off to $5.2 \pm 1.4 \times 10^{-18}$ ergs s^{-1} cm^{-2} arcsec^{-1} in a 2″ × 2″ square $\sim 70\ h_{50}^{-1}$ kpc off-nucleus. The faintest Hα surface brightness associated with the 2A0335+096 nebular system is $4.5 \pm 0.26 \times 10^{-18}$ ergs s^{-1} cm^{-2} arcsec^{-1} in a 2″ × 2″ square $\sim 24\ h_{50}^{-1}$ kpc away from the bright nucleus. In PKS 0745−191, the nebular region seems to have a harder "edge"; we could have detected emission $\sim$3 times fainter in a 2″ × 2″ box, but we did not. The Hα surface brightness of the nebula in PKS 0745−191 drops below detectable limits at $\sim 26\ h_{50}^{-1}$ kpc at a surface brightness of $\sim 1.2 \pm 0.14 \times 10^{-17}$ ergs s^{-1} cm^{-2} arcsec^{-1}. The equivalent width of the emission there is $\sim$10 Å and would be detectable even if it were fainter.

TABLE 1

SURFACE BRIGHTNESS LIMITS ON OPTICAL EMISSION LINES

Cluster	Projected Radius (h_{50}^{-1} kpc)	Hα[a]	[Fe X] 6374 Å[a]
PKS 0745−191.....	65	1.9×10^{-18}	1.9×10^{-18}
PKS 0745−191.....	115	1.7×10^{-18}	2.1×10^{-18}
A1795.....	93	3.9×10^{-18}	3.5×10^{-18}
2A0335+096.....	43	2.7×10^{-18}	2.7×10^{-18}

[a] In units of ergs cm^{-2} s^{-1} arcsec^{-2}.

5.2. *X-Ray/Optical Connection*

Apparently, X-ray absorption in clusters of galaxies does not come from gas-phase metals in ionized, atomic, or molecular gas. We now consider whether the absorption can come from metals in solid state form. Dust grains with a Mathis, Rumpl, & Nordsieck (1977) size distribution absorb soft X-ray photons and optical photons with about equal efficiency (e.g., Laor & Draine 1993). If grains are responsible for the X-ray absorption, we would expect them to cause a comparable amount of optical extinction.

The evidence for optical extinction associated with clusters is tantalizing but inconclusive. There appear to be deficits of distant galaxies (Zwicky 1957; Karachentsev & Lipotvetskii 1969; Bogart & Wagoner 1973; Szalay, Hollosi, & Toth 1989) and quasars (Boyle, Fong, & Shanks 1988; Romani & Maoz 1992) behind clusters of galaxies. The implied area-averaged extinctions range from $A_B \sim 0.2$ mag (Boyle et al. 1988) to $A_B \sim 0.5$ (Romani & Maoz 1992). Because these surveys indicate extinction extending over projected radii greater than 1 Mpc at the distance of the cluster, absorbing dust would have to be present well outside the cooling-flow regions of clusters and should produce a similarly extended soft X-ray absorption signature. In Galactic dust, $A_B \sim 0.4$ corresponds to a color excess $E(B-V) \sim 0.1$ (Spitzer 1978). Dust of this kind distributed through the ICM of a cluster would cause a dispersion in $E(B-V)$ among otherwise identical cluster members. Ferguson (1993) has analyzed the colors of 130 elliptical galaxies in 19 clusters and 256 elliptical galaxies in poor groups and the field and finds that the excess reddening in clusters can be no greater than $E(B-V) = 0.06$.

Dust in the intracluster medium, however, might be quite unlike Galactic dust. Sputtering in a hot ICM of density $n_{\rm H}$ destroys grains a_μ μm in size in $\sim(6 \times 10^{13}$ s cm$^{-3})n_{\rm H}^{-1}a_\mu$ (Draine & Salpeter 1979). Small grains disappear first, and all grains smaller than 1 μm sputter away in less than a Hubble time if $n_{\rm H} > 10^{-4}$ cm^{-3}. These grains will only be long-lived at the outskirts of the cluster, far from the cooling flow. In Galactic dust, the X-ray opacity comes mostly from large grains, while the UV opacity comes mostly from small grains. When only those grains larger than 0.1 μm are left, the extinction curve is grayer than Galactic, and a given amount of extinction produces much less reddening.

5.3. *Dust Optical Depths in the ICM*

The ICM density outside the cluster core radius $r_c \sim 200$ kpc typically declines proportional to $[1 + (r/r_c)^2]^{-1}$ (e.g., Sarazin 1988). To simplify the following calculations, we will ignore the fact that central densities in cooling-flow clusters continue to rise inside r_c. The hydrogen column density through the center of a cluster with this density profile is $N_H \sim (1.6 \times 10^{21}$ cm$^{-2})n_{-3}r_{200}$, where n_{-3} is the central electron density in 10^{-3} cm^{-3} and $r_{200} = r_c/(200$ kpc). At this column density, Galactic extinction produces optical depths $\sim 0.5n_{-3}r_{200}$ at 5000 Å and $\sim 0.3n_{-3}r_{200}$ at 400 eV (Laor & Draine 1993).

Large grains contain most of the dust mass and are therefore responsible for the bulk of the X-ray and optical absorption. The optical depth of large grains in the ICM can be estimated assuming that grains of radius a_μ μm contain a fraction $0.01\chi_d$ of the ICM mass in solid state form with a density of ~ 2 g cm^{-3}. The geometrical cross section per H atom is then $\sim(6.3 \times 10^{-23}\ \mathrm{cm}^2)\chi_d a_\mu^{-1}$, giving a geometrical optical depth $\sim 0.10\chi_d a_\mu^{-1} n_{-3} r_{200}$. The absorption cross sections of large grains ($\gtrsim 0.3$ μm) from the optical through the soft X-ray band are similar to their geometrical cross sections (Laor & Draine 1993). Grains with $a_\mu \sim 0.3$ produce optical and X-ray opacities similar to the values for Galactic dust.

The mass column density in grains needed for marginal optical thickness in both bands is $\sim 10^{-4}$ g cm^{-3}. Over the central 1 Mpc of the cluster, the total dust mass implied by optical/X-ray absorption is $\sim 10^{12}\ M_\odot$, similar in magnitude to the total mass of metals in the entire cluster. Such a large dust mass is theoretically unpalatable, but it cannot be ruled out categorically.

5.4. *Far-Infrared Continuum Limits*

Electrons in the hot ICM collisionally heat dust grains, causing them to radiate in the far-infrared and submillimeter bands. In plasmas hotter than $\sim 3 \times 10^7$ K, the equilibrium dust temperature (T_d) depends primarily on electron density because dust grains are marginally transparent to hot electrons (Dwek 1987; Dwek, Rephaeli, & Mather 1990). Dwek (1987) finds $T_d \approx 15 n_{-3}^{0.18}$ K. Gas at ICM temperatures thus cools at the rate $n_e n_{\rm H} \Lambda_d \chi_d$, where $\Lambda_d = 3\text{–}6 \times 10^{-21}$ ergs cm^3 s^{-1} and χ_d is the dust-to-gas ratio in Galactic units (Dwek 1987). The low end of this range applies when all the grains are large. The infrared luminosity from the ICM when χ_d is constant is then $\sim(5.0 \times 10^{45}\ \mathrm{ergs\ s^{-1}}) n_{-3}^2 \chi_d r_{200}^3$, where $r_{200} = r_c/(200\ \mathrm{kpc})$.

Dust with $\chi_d \sim 1$ at $r < r_c$ would radiate copiously at 100 μm and would exacerbate the "mass sink problem" by a factor of order 10^2 (Dwek et al. 1990; Hu 1992; Bregman 1992). Within the cores of cooling-flow clusters, $n_{-3} > 3$. The far-IR luminosity then exceeds $(4.5 \times 10^{46}\ \mathrm{ergs\ s^{-1}})\chi_d r_{200}^3$ and, at $T_d \sim 20$ K, falls largely within the IRAS 100 μm band (Dwek et al. 1990). *IRAS* observations toward the central dominant galaxies of clusters find far-IR luminosities of $\sim 10^{44}$–10^{45} ergs s^{-1} (Bregman, McNamara, & O'Connell 1990; Grabelsky & Ulmer 1990), implying $\chi_d \lesssim 10^{-2}$. Hence, ICM dust within the cluster core cannot be marginally optically thick.

If dust is continually injected into the ICM, sputtering maintains $\chi_d \lesssim 10^{-2}$ at the center of the cluster, but as the ICM density drops with radius, sputtering decreases, and χ_d can rise (Dwek et al. 1990; Hu 1992). At $r > r_g \equiv 3 r_c n_{-3}^{1/2}$, the ICM electron density is lower than 10^{-4} cm^{-3}, and large grains can survive for longer than 10^9 yr. Following Hu (1992), let us assume, somewhat arbitrarily, that $\chi_d \propto n_{\rm H}^{-1}$ inside r_g and $\chi_d = \chi_{d0} = $ const. outside r_g. Then the dust luminosity from $r < r_g$ is

$$(2.2 \times 10^{45}\ \mathrm{ergs\ s^{-1}}) n_{-3}^{3/2} r_{200}^3 \chi_{d0} \left(1 - \frac{\tan^{-1} 3 n_{-3}^{1/2}}{3 n_{-3}^{1/2}}\right),$$

and the luminosity from $r > r_g$ is

$$(3.2 \times 10^{45}\ \mathrm{ergs\ s^{-1}}) n_{-3}^2 r_{200}^3 \chi_{d0} \times \left(\frac{\pi}{2} - \frac{3 n_{-3}^{1/2}}{1 + 9 n_{-3}} - \tan^{-1} 3 n_{-3}^{1/2}\right).$$

Since the typical dust temperature at r_g is ~ 10 K, the bulk of this flux emerges longward of the *IRAS* 100 μm band. The 5000 Å dust optical depth through the entire cluster is

$$\sim \left(0.1 + 0.1 n_{-3} \frac{\pi/2 - \tan^{-1} 3 n_{-3}^{1/2}}{\pi/2 - \tan^{-1} 3}\right) \chi_{d0} r_{200}.$$

Although interstellar cirrus severely complicates measurements of far-IR fluxes from clusters (e.g., Wise et al. 1993), Hu (1992) has shown that dust can exist at $r \sim r_g$ in quantities sufficient to produce the optical extinction without overproducing *IRAS* 100 μm flux.

Submillimeter continuum observations might soon be able to confirm or deny the presence of intracluster dust with large column densities. Current estimates of the opacity of Galactic grains at 1 mm are inexact, ranging over more than an order of magnitude centered on $\sim 10^{-2}$ cm^2 g (Draine 1990), about 10^{-4} times the optical/soft X-ray opacity. Adopting this value gives a continuum brightness temperature of ~ 1 mK for a layer of 10 K dust with a 5000 Å optical depth of unity. Annis & Jewitt (1993) have limited the 0.8 and 1.1 mm fluxes over an 18″ beam at the centers of 11 clusters to <12–60 mJy at the 3 σ level, corresponding to brightness temperature limits of <0.7–3.5 mK. However, their chopping technique does not allow them to detect continuum flux distributed over more than 100 kpc.

6. SUMMARY

Some cooling-flow clusters of galaxies appear to contain soft X-ray–absorbing material with $N_{\rm H} \sim 10^{21}$ cm^{-2} partially covering the central 100 kpc or more. The corresponding mass of $\sim 10^{12}\ M_\odot$ is comparable to the amount that would condense out of a 100 $M_\odot$ yr^{-1} cooling flow over a Hubble time, prompting suggestions that the absorbing clouds are cooling-flow condensates. Whatever absorbs the X-rays must reradiate an equivalent flux somewhere in the electromagnetic spectrum, but identifying the absorbing material has proven to be quite difficult.

In atomic cooling-flow clouds, in which infrared fine-structure line cooling balances X-ray heating, the H I 21 cm line becomes optically thick in a layer at a temperature of ~ 20 K. If we assume thermal line widths, the 21 cm line fluxes from the surfaces of these clouds are minimized. Nevertheless, current 21 cm observations constrain the covering factors of such clouds to be less than 0.1. To avoid 21 cm detection, cold intracluster clouds with a high enough covering factor to produce the X-ray absorption must be molecular. Dust is needed to catalyze molecule formation in X-ray–irradiated clouds. Since dust grains form from molecules, it is extremely difficult to form dust, and therefore molecules, at $N_{\rm H} \lesssim 10^{21}$ cm^{-2} in pristine clouds that have condensed out of a dust-free ICM, although "seed dust" can promote the formation of additional dust.

Molecular clouds in the ICM radiate CO $J = 1$–0 lines that are least detectable when the line widths are thermal. Flux balance requires molecular cloud temperatures to be ~ 20 K, and current CO observations constrain the covering factors of these clouds also to be less than 0.1. These limits relax somewhat if more than 99% of the CO condenses onto dust, but X-ray transient heating of small grains and spot heating of grain surfaces prevent such complete condensation. Apparently the covering factors of cold clouds, be they atomic or molecular, are too small to produce the observed soft X-ray

absorption. These low covering factors do not necessarily eliminate the possibility that large amounts of material condense out of cooling flows into cold clouds. At a characteristic Jeans column density of 3×10^{22} cm^{-2}, a condensed mass of 10^{12} $M_\odot$ covers $\sim 3.5 \times 10^3$ kpc^2 or about 3% of a region 200 kpc in radius.

The hot ICM itself is too highly ionized to absorb soft X-rays but could be more opaque at $\lesssim 1$ keV if it contained a cooler ionized component or dust grains. Line emission from ionized gas with $N_H \sim 10^{21}$ cm^{-2} in pressure equilibrium with the cooling-flow region would be extremely luminous. Spectroscopy of optical emission lines rules out ionized absorbing gas at less than 1.5×10^6 K, ASCA spectra rule out ionized absorbing gas at $1.5–3 \times 10^6$ K, and hotter gas would be too highly ionized to absorb soft X-rays significantly.

Dust in the ICM is one possibility we cannot rule out. Dust absorbs soft X-rays and optical photons with comparable efficiencies. Background counts of galaxies and quasars behind clusters of galaxies are consistent with optical depths in both the optical and soft X-ray bands of 0.2–0.5. The necessary amount of obscuring dust cannot lie entirely inside the cores of clusters without producing a 100 μm flux that would have been detected by *IRAS*, so it must be distributed more widely throughout the ICM. If dust is indeed responsible for soft X-ray absorption in clusters, then there should be some excess absorption away from the cluster core, and the spectral dependence of soft X-ray extinction should be flatter than that of purely gaseous absorbing material. The required dust mass, $\sim 10^{12}$ $M_\odot$, comparable to the entire metal content of a cluster, is uncomfortably large but not impossibly large. Continuum emission from this large a dust mass, spread over the central ~ 1 Mpc of a cluster, lies near the current limits of submillimeter detectability.

The authors thank the Virginia Institute for Theoretical Astrophysics for sponsoring the visit during which this work was initiated. We thank Chris McKee and Craig Sarazin for their valuable input early on and Chris O'Dea, Stefi Baum, and Brian McNamara for numerous discussions concerning radio and submillimeter observations of cooling-flow clusters. This work was supported by NASA through grant number HF-1054.01-93 from the Space Telescope Science Institute, which is operated by the Association of Universities for Research in Astronomy, Inc., under NASA contract NAS 5-26555.

REFERENCES

Allen, S. W., Fabian, A. C., Johnstone, R. M., White, D. A., Daines, S. J., Edge, A. C., & Stewart, G. C. 1993, MNRAS, 262, 901
Annis, J., & Jewitt, D. 1993, MNRAS, 264, 593
Antonucci, R., & Barvainis, R. 1994, AJ, 107, 448
Bogart, R. S., & Wagoner, R. V. 1973, ApJ, 181, 609
Boyle, B. J., Fong, R., & Shanks, T. 1988, MNRAS, 231, 897
Braine, J., & Dupraz, C. 1994, A&A, 283, 407
Braine, J., Wyrowski, F., Radford, S. J. E., Henkel, C., & Lesch, H. 1995, A&A, 293, 315
Bregman, J. N. 1992, in Clusters and Superclusters of Galaxies, ed. A. C. Fabian (Dordrecht: Kluwer), 119
Bregman, J. N., & Hogg, D. E. 1988, AJ, 96, 455
Bregman, J. N., McNamara, B. R., & O'Connell, R. W. 1990, ApJ, 351, 406
Bregman, J. N., & Roberts, M. 1990, ApJ, 362, 468
Burns, J. O., White, R. A., & Haynes, M. P. 1981, AJ, 86, 120
Cowie, L. L., & Binney, J. J. 1977, ApJ, 215, 723
Cravens, T. E., Victor, G. A., & Dalgarno, A. 1975, Planet. Space Sci., 23, 1059
Crawford, C. S., & Fabian, A. C. 1993, MNRAS, 265, 431
Daines, S. J., Fabian, A. C., & Thomas, P. A. 1994, MNRAS, 268, 1060
Donahue, M., & Stocke, J. T. 1994, ApJ, 422, 459
Donahue, M., & Voit, G. M. 1991, ApJ, 381, 361
———. 1993, ApJ, 414, L17
Draine, B. T. 1990, in The Interstellar Medium in Galaxies, ed. H. A. Thronson & J. M. Shull (Dordrecht: Kluwer), 473
———. 1995, in The Physics of the Interstellar Medium and Intergalactic Medium, ed. A. Ferrara, C. F. McKee, C. Heiles & P.R.Shapiro (San Francisco: ASP), 133
Draine, B. T., & Lee, H. M. 1984, ApJ, 285, 89
Draine, B. T., & Salpeter, E. E. 1979, ApJ, 231, 77
Dwakaranath, K. S., van Gorkom, J. H., & Owen, F. N. 1994, ApJ, 432, 469
Dwek, E. 1987, ApJ, 322, 812
Dwek, E., Rephaeli, Y., & Mather, J. C. 1990, ApJ, 350, 104
Fabian, A. C. 1994, ARA&A, 32, 277
Fabian, A. C., Arnaud, K. A., Bautz, M. W., & Tawara, Y. 1994, ApJ, 463, L63
Fabian, A. C., Johnstone, R. M., & Daines, S. J. 1994, MNRAS, 271, 737
Fabian, A. C., & Nulsen, P. E. J. 1977, MNRAS, 180, 479
Ferguson, H. C. 1993, MNRAS, 263, 343
Ferland, G. J. 1993, University of Kentucky Department of Physics and Astronomy Internal Rep.
Ferland, G. J., Fabian, A. C., & Johnstone, R. M. 1994, MNRAS, 266, 399 (FFJ)
Glassgold, A. E., & Langer, W. D. 1973, ApJ, 186, 859
Goldreich, P., & Kwan, J. 1974, ApJ, 189, 441
Goldsmith, P. F., & Langer, W. D. 1978, ApJ, 222, 881
Grabelsky, D. A., & Ulmer, M. P. 1990, ApJ, 355, 401
Habing, H. J. 1968, Bull. Astr. Inst. Netherlands, 19, 421
Heckman, T. M., Baum, S. A., van Breugel, W. J. M., & McCarthy, P. J. 1989, ApJ, 338, 48
Henry, R. J. W., & Lane, N. F. 1969, Phys. Rev., 183, 221
Hollenbach, D., & McKee, C. F. 1979, ApJS, 41, 555
———. 1989, ApJ, 342, 306
Hu, E. 1992, ApJ, 391, 608
Jaffe, W. 1992, in Clusters and Superclusters of Galaxies, ed. A. C. Fabian (Kluwer: Dordrecht), 109
Jones, A. P., Tielens, A. G. G. M., Hollenbach, D. J., & McKee, C. F. 1994, ApJ, 433, 797
Jura, M. 1987, in Interstellar Processes, ed. D. J. Hollenbach & H. A. Thronson (Dordrecht: Reidel), 3
Karachentsev, I. D., & Lipovetskii, V. A. 1969, Soviet Astron., 12, 909
Laor, A., & Draine, B. T. 1993, ApJ, 402, 441
Lazareff, B., Castets, A., Kim, D. W., & Jura, M. 1989, ApJ, 336, L13
Leger, A., Jura, M., & Omont, A. 1985, A&A, 144, 147
Maloney, P., & Black, J. H. 1988, ApJ, 325, 389
Mathis, J. S., Rumpl, W., & Nordsieck, K. H. 1977, ApJ, 217, 425
McNamara, B. R., Bregman, J. N., & O'Connell, R. W. 1990, ApJ, 360, 20 (MBO)
McNamara, B. R., & Jaffe, W. 1994, A&A, 281, 673
McNamara, B. R., & O'Connell, R. W. 1992, ApJ, 393, 579
Mirabel, F., Sanders, D. B., & Kazes, I. 1989, ApJ, 340, L9
O'Dea, C. P., Baum, S. A., Maloney, P. R., Tacconi, L. S., & Sparks, W. B. 1994, ApJ, 422, 467 (OBMTS)
O'Dea, C. P., Gallimore, J. F., & Baum, S. A. 1995, AJ, 109, 26
O'Dea, C. P., & Payne, H. 1991, BAAS, 23, 1338
———. 1995, in preparation
Pistinner, S., & Sarazin, C. L. 1994, ApJ, 433, 577
Romani, R. W., & Maoz, D. 1992, ApJ, 386, 36
Sarazin, C. L. 1988, X-Ray Emission from Clusters of Galaxies (Cambridge: Cambridge University Press)
Scoville, N. Z., & Solomon, P. M. 1974, ApJ, 187, L67
Seab, C. G. 1987, in Interstellar Processes, ed. D. J. Hollenbach & H. A. Thronson (Dordrecht: Reidel), 491
Shull, J. M. 1978, ApJ, 219, 877
Shull, J. M., & Beckwith, S. 1982, ARA&A, 20, 163
Shull, J. M., & Van Steenberg, M. E. 1982, ApJS, 48, 95
———. 1985, ApJ, 298, 268
Sparks, W. B., Macchetto, F., & Golombek, D. 1989, ApJ, 345, 153
Spitzer, L. 1978, Physical Processes in the Interstellar Medium (New York: Wiley-Interscience)
Szalay, A. S., Hollosi, J., & Toth, G. 1989, ApJ, 339, L5
Tielens, A. G. G. M., & Hollenbach, D. 1985, ApJ, 291, 722
Tielens, A. G. G. M., McKee, C. F., Seab, C. G., & Hollenbach, D. J. 1994, ApJ, 431, 321
Valentijn, E. A., & Giovanelli, R. 1982, A&A, 114, 208
Voit, G. M. 1991a, ApJ, 377, 158
———. 1991b, ApJ, 379, 122
Voit, G. M., Donahue, M., & Slavin, J. D. 1994, ApJS, 95, 87
White, D. A., Fabian, A. C., Johnstone, R. M., Mushotzky, R. F., & Arnuad, K. A. 1991, MNRAS, 252, 72
Wise, M. W., O'Connell, R. W., Bregman, J. N., & Roberts, M. S. 1993, ApJ, 405, 94
Xu, Y., & McCray, R. 1991, ApJ, 375, 190
Zwicky, F. 1957, Morphological Astronomy (Berlin: Springer)